bulk solids handling Journal

Research Paper

Load Stability of Bulk Cargoes during Ship Transport

Edited by on 11. Nov. 2019
Published in bulk solids handling, Vol. 34 (2014) No. 1

The safe ocean transport of bulk cargoes on large bulk ships is vitally dependent on the stability of the cargo under the influence of the rolling, pitching and yawing motion of the ship and the transmission of vibration from the ship's engine and propulsion machinery as well as wave motion induced whipping. Safety standards for ship transport are set by such bodies as the International Maritime Organisation with recommended tests for the assessment of bulk ores deemed suitable for safe ship transport. These test procedures are somewhat empirical and take no account of the well established and proven flow property tests, analysis and design methodologies widely accepted in field of bulk solids handling. These matters are discussed in this article. The stress states in loaded bulk cargoes are examined with respect to the establishment of maximum limits for surface rill angles as a function of a ship's roll angles.

It is most important that the stability of the loaded bulk cargo on a vessel be guaranteed under all dynamic conditions. (Picture: PF-SELF)

Introduction

A subject of particular importance to the resources industries concerns the safe, intercontinental, bulk ship trans-ocean transport of large tonnages of bulk ores such as coal and mineral concentrates. It is most important that the stability of the loaded bulk cargo be guaranteed under all dynamic conditions due to the rolling and pitching motion of the vessel and the vibration influence emanating from the ship’s engines, propulsion equipment as well as whipping motion induced by waves.

While the reported incidences of cargo slip and movement leading to the capsizing and sinking of bulk carriers has significantly reduced in recent years, the problem of ensuring that stringent safety standards are met is a matter of paramount importance. This objective is strongly reinforced by the fact that transportation tonnages are increasing significantly and bulk ships are becoming much larger.

Currently, the safe ship transport of bulk cargoes is controlled, primarily, by the International Maritime Organisation (IMO) with reference to the “International Maritime Solid Bulk Cargoes (IMSBC) Code” [1]. This quite detailed publication includes test procedures, such as the tests for the determination of safe Transportable Moisture Limit (TML), which include the Flow Table Test, Penetration Test and Proctor/Fagerberg Test. In general, there appear to be elements of empiricism in these tests and there is no evidence of any reference to the now well established flow property tests that are an integral part of design and performance evaluation of industrial bulk solids handling plant. Furthermore, the wealth of knowledge that is now accumulated in the field of bulk solids handling has great potential for improving the knowledge and understanding of bulk cargo stability for safe transportation of bulk ores.

With this background, the purpose of this article is to briefly review the current practice adopted by the IMO and indicate areas where the recognised bulk solids test procedures may be applied, such as in the measurement of bulk strength, internal and boundary friction angles, bulk density variation with consolidation stress and moisture and fines migration under the influence of vibration. The main focus of the article will be on the stress states that exist in bulk solids stored in a ship’s hold and the generation of slip surfaces that could occur under the rolling and pitching action of the ship. The article is based on the original of work

Roberts and Scott [2] of the University of Newcastle Australia and by Kirby [3] of the Warren Spring Laboratory.

1. International Maritime Organisation (IMO) Recommended Tests

Of particular importance with respect to vessel stability are bulk cargoes that may liquefy, generating slip planes that may cause the cargo to shift. This emphasises the need to establish the safe TML for bulk solids that are to be transported by ship. The IMSBC Code refers to the following three testing methods [1].

1.1 Flow Table Test

As stated by the IMSBC Code, this test “is generally suitable for mineral concentrates or other fine material with a maximum grain size of 1 mm [1]. It may also be used for other materials with a maximum grain size of 7 mm. It will not be suitable for materials coarser than this and may also not give satisfactory results for some materials with a high clay content. If the flow table test is not suitable for the material in question, the procedures adopted should be those approved by the authority of the port state”.

The test provides for the determination of the

- the Flow Moisture Point (FMP) of the material under impact or cyclical forces of the flow table apparatus,
- moisture content of the cargo, and
- the Transportable Moisture Limit (TML) of the test material.

1.2 Penetration Test

As stated by the IMSBC Code, this test “constitutes a procedure whereby a material in a cylindrical vessel is vibrated [1]. The flow moisture point is determined on the basis of the penetration depth of an indicator”.

The following relevant information is also given:

- The test is generally suitable for mineral concentrates, similar materials, and coals up to a top size of 25 mm.
- The sample, in a cylindrical vessel, is subjected to vertical vibration of 2 g rms ± 10% for 6 minutes.

- When the penetration depth of a bit put on the surface exceeds 50 mm, it is judged that the sample contains a moisture content greater than the flow moisture point.

1.3 Proctor/Fagerberg Test

The Proctor Fagerberg test has its origin derived from soil mechanics, with Proctor developing a method for control of the compaction of cores of earth dams and road sub-bases [4]. In this work it was shown that the dry density of a soil at a given compactive effort depends on the amount of water contained in the soil. The method applies a standard amount of energy via a falling weight hammer to moist soil placed in three layers (for the standard Proctor test) in a mould of standard dimensions.

As stated by the IMSBC Code, the scope of this test includes:

- Test method for both fine and relatively coarse-grained ore concentrates or similar materials up to a top size of 5 mm. This method must not be used for coal or other porous materials.
- Before the Proctor/Fagerberg test is applied to coarser materials with a top size greater than 5 mm, an extensive investigation for adoption and improvement is required.
- The TML of a cargo is taken as equal to the critical moisture content at 70% degree of saturation according to the Proctor/Fagerberg method test.

1.4 Method Comparison

When comparing test results obtained for the same bulk material cargo using the three IMO testing methods, a noticeable difference in the results is often observed, which may create some doubt over the validity of the testing methods and how applicable they are for a given bulk material.

2. Relevant Test for Determination of Bulk Solids Flow Properties

The apparent empirical nature of the foregoing IMO tests makes it difficult to see how they relate to the actual physical conditions applying in a bulk ship. On the other hand, in the field of bulk solids handling, the test procedures and design methodologies are closely related and well proven. The possible application of these procedures to bulk cargo transportation need to be explored. The relevant tests are briefly reviewed.

2.1 Flow Properties Tests

Focusing specifically on bin, hopper, stockpile, feeders, transfers and conveyors design, the laboratory tests aim to duplicate field conditions and provide the designer with such parameters as:

- Yield loci and flow functions for instantaneous and time storage conditions for the range of moisture contents and, as relevant, temperatures occurring in practice. The flow functions represent the variation of unconfined yield strength $?_c$ with major consolidation stress $?_1$ as occurs during storage and flow.
- Effective angle of internal friction ? as a function of major consolidation stress.
- Static angle of internal friction φ_t as a function of major consolidation stress and time consolidation.
- Wall friction angles φ as a function of normal stress for different bin and chute wall materials and finishes.
- Bulk density ? as a function of major consolidation stress.

The foregoing tests are based on the original work of Jenike [5] and have been subsequently documented by others such as by Roberts [6]. A typical set of flow property graphs for a sample of coal are shown in Figs. 1, 2 and 3.

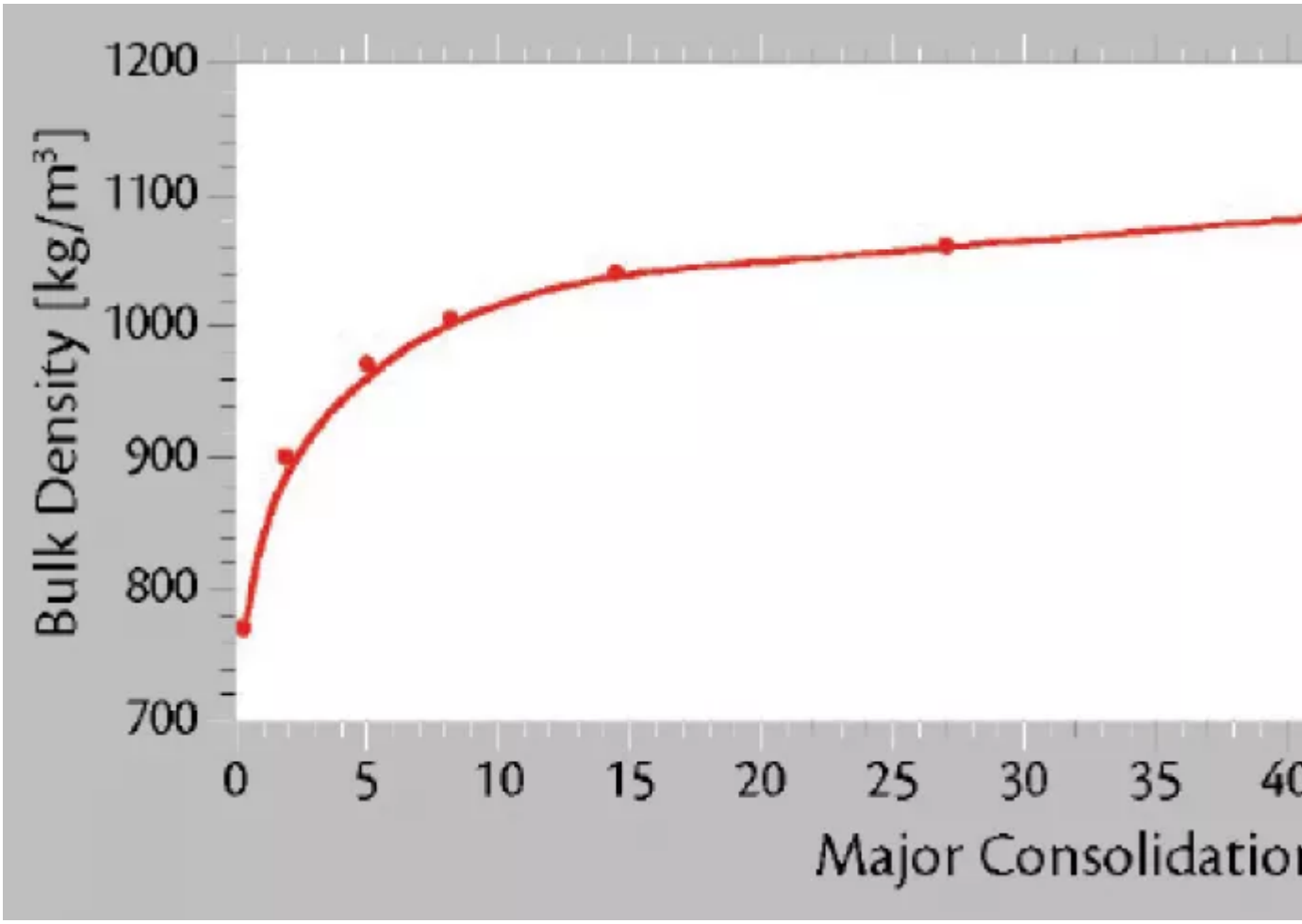

Fig. 1: Graphs showing the relation between major consolidation stress and bulk dens
sample of coal.

2.2 Effect of Moisture on Bulk Strength and Density

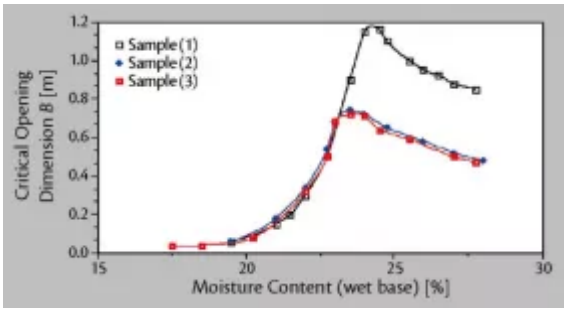

Fig. 4: Critical cohesive arching dimension of coal as a function of moisture content.

Changes in moisture content can significantly influence the strength of bulk solids. By way of illustration, the critical cohesive arching dimension *B* for a stainless steel lined hopper containing three Hunter Valley coals plotted as a function of moisture content are shown in Fig. 4.

Sample (1) is a raw open cut coal, Sample (2) a washed version of Sample (1), and Sample (3) a blend of Sample (2) with another washed coal. The high strength of Sample (1) is clearly evident. Experience has shown that the peak bulk strength of virtually all bulk solids including coal may occur at a moisture content somewhere between 70 and 90% of the saturation limit. Washed coals such those illustrated by curves of Samples (2) and (3) in Fig. 3 generally exhibit very little, if any, increase in bulk strength due to time storage.

Bulk density tests performed on many coal types have shown that, almost invariably, the bulk density is a minimum at the moisture content for which the bulk strength is a maximum. This is illustrated for a coal sample in Figs. 5 and 6.

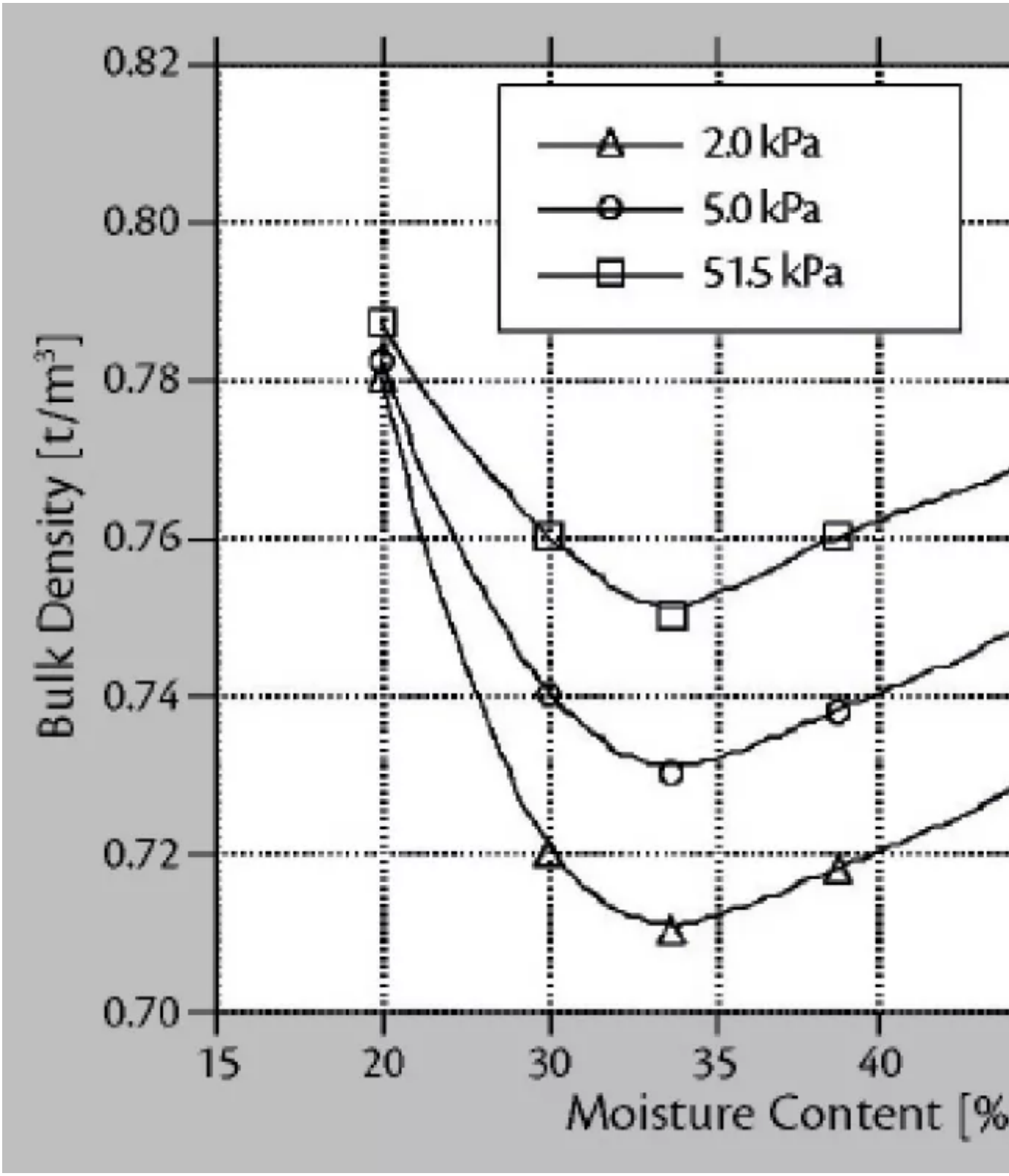

Fig. 5: Influence of moisture content on bulk density for a coal sample.

2.3 Effect of Vibrations on Strength and Flow

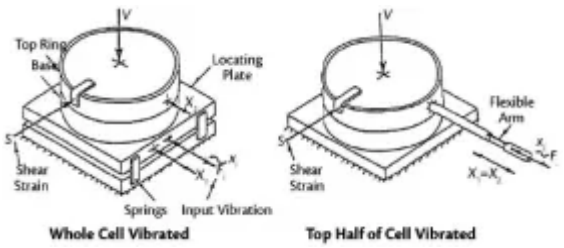

Fig. 7: Vibrated shear cell.

The application of mechanical vibrations to promote gravity flow of bulk solids has been studied by Roberts [7]. A dynamic shear test apparatus was developed which allows vibrations to be applied to a shear cell as shown in Fig. 7. The tests permit the shear strength to be determined in the presence of vibrations which may be applied over a range of amplitudes and frequencies.

The strength of bulk solids is measured in terms of the unconfined yield strength σc which is related to the major consolidation pressure σ_1 by the yield locus and Mohr diagram as illustrated in Fig. 8. This Figure shows two yield loci, a non-vibrated yield locus for which the unconfined yield strength σ_c corresponds to the major consolidation pressure σ_1. For the same consolidation conditions, the application of vibrations during shear leads to the vibrated yield locus and the unconfined yield strength σ_{cf}. The unconfined yield strengths σc and σcf give one point on the respective flow functions shown in Fig. 9. A family of yield loci, for at least three consolidation conditions, needs to be obtained for the complete flow functions of Fig. 9 to be determined.

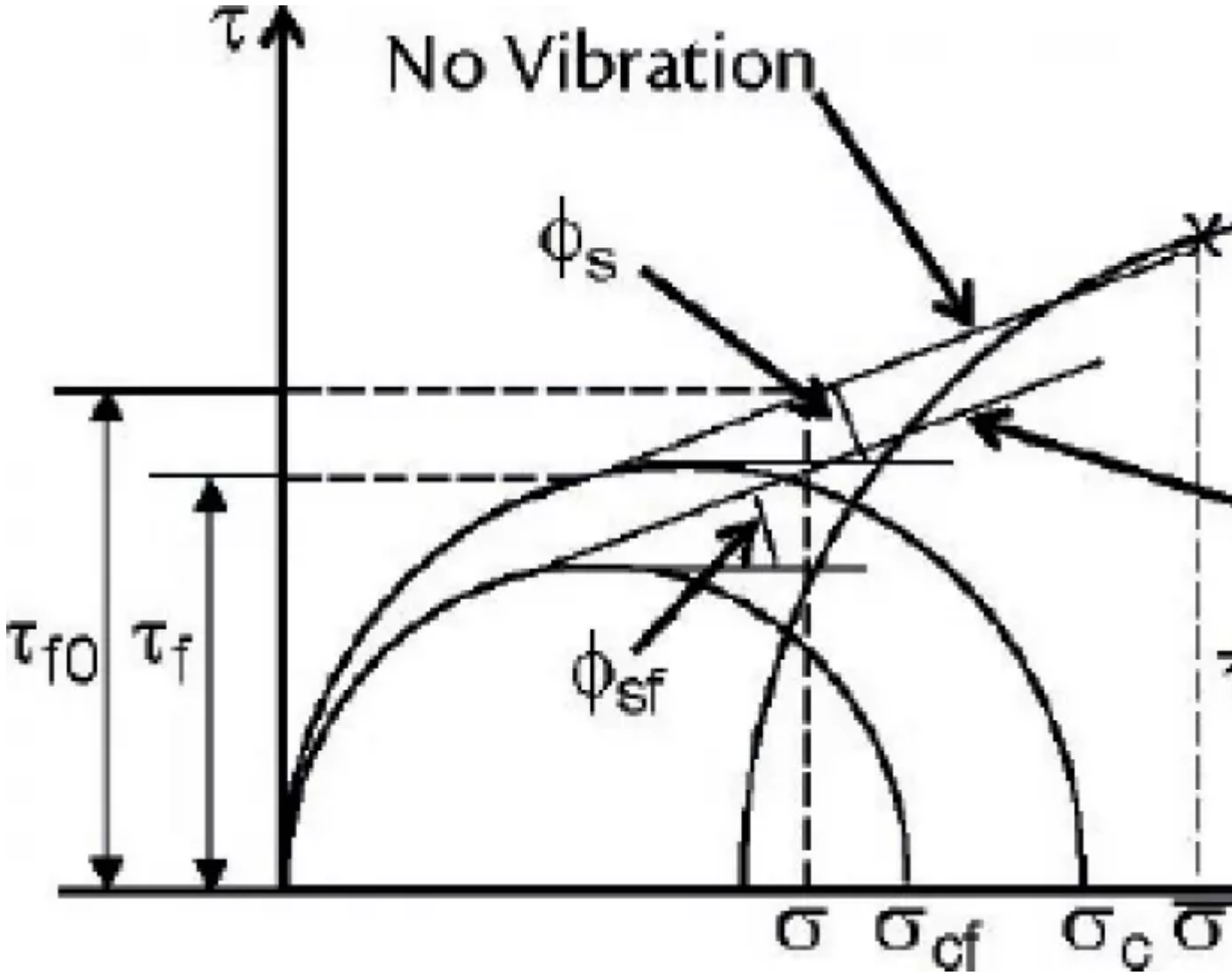

Fig. 8: Vibrated yield loci.

It has been shown that the dynamic shear strength decays exponentially with increase in vibration velocity in accordance with the relation:

$$\tau_f = \tau_{f0} \cdot \left[\frac{\tau_\infty}{\tau_{f0}} + \left(1 - \frac{\tau_\infty}{\tau_{f0}} \right)^{-\frac{2 \cdot \pi \cdot X_r \cdot f}{U}} \right]$$

where:

- ƒ is the frequency (Hz), and
- τ_∞ is a constant, and
- *U* is another constant.

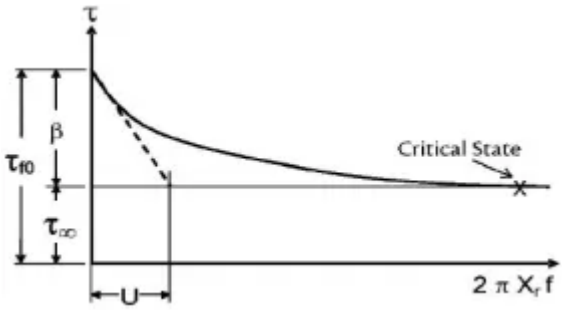

Fig. 10: Shear stress vs. vibration velocity.

For a given solids, the constants τ_∞ and *U* depend on the consolidation and normal pressure applied during shear.

The decay in shear strength is illustrated in Fig. 10. The constant *U* in Eq. (1) is referred to as the bulk solid vibration velocity constant.

Experimental evidence to date suggests that *U* is independent of the consolidation pressure and applied normal pressure. By way of example, *U* is approx. 7 mm/s for a refractory clay pyrophyllite and 10 mm/s for a typical iron ore. If *U* is known for the particular bulk solid, the values of relative amplitude X_r and frequency ƒ for maximum reduction in shear strength may be estimated from Eq. (2):

$$X_r \cdot f \geq 0.8 \cdot U$$

It should be noted that the decay in shear strength with vibration velocity as described above is similar to the decay in shear strength with voidage on the shear plane. This implies that the vibration velocity (or energy) is directly related to the voidage.

3. Stability of Bulk Solids during Ship Transport

3.1 Load Profiles

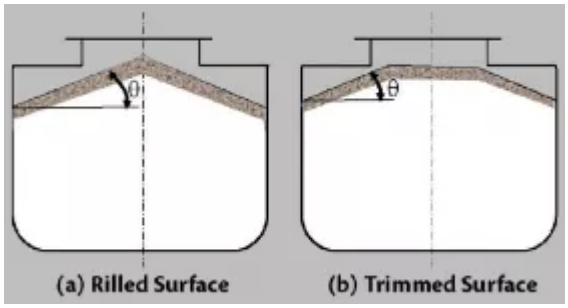

Fig. 11: Cross section of loaded cargo hold.

Generally, the bulk solid in the hold of an ore carrier is constrained on three boundaries with only the top surface free, as indicated in Fig. 11. The load profile depends on the shape of the hold, the hatch arrangement and degree of fill. Depending on the manner in which the bulk solid is loaded, the surface will normally be rilled, as in Fig. 11(a) with the surface inclined at an angle equal to or less than the angle of repose as a result of the settling process during the initial phase of the ship’s journey. Some trimming of the surface may be effected as in Fig. 11(b), and this is desirable for stability purposes.

It is assumed that the moisture content of the bulk solid is below the saturation (water holding capacity) level and, as such, the bulk solid can be described as a Coulomb frictional, cohesive bulk solid. The bulk solid will consolidate during initial filling, the consolidation continuing with time under constrained storage. Depending on the properties of the bulk solid, some chemical bonding of particles may occur over prolonged undisturbed storage leading to a further increase of bulk strength. Consolidation will be further promoted by the ship’s vibrations, those emanating from the engines and other machinery, and those of a lower frequency due to the ship’s motion. On some occasions, the latter may lead to a reduction in strength if significant downward accelerations occur, mainly during

rolling and pitching. These effects may lead to some movement of the mass but, in general, this will be confined to the region adjacent to the free surface where the bulk mass is unconstrained. The bulk of the stored mass is constrained by the walls and floor where the combination of wall friction and pressures will prevent or limit relative motion with respect to the walls of the hold.

The angle of repose, θ, of the free surface is on occasions confused with the angle of internal friction. The angle of repose is simply the angle with respect to the horizontal formed when a bulk solid is placed into storage and depends on the loading rate, impact due to loading and the particle/lump size distribution. The angle of repose may be thought of as the angle of internal friction of a loosely packed unconsolidated stored mass. During filling it is common for some segregation to occur, with the fines remaining in the central region and the larger lumps rolling to the sides. Under these conditions the surface may have a range of slopes, being steeper in the central region due to cohesion of the fines and less steep at the outsides due to the more free-flowing nature of the lumps. Where the bulk mass has a more uniform size distribution, the surface will tend to slope at a constant angle with some settlement of the surface due to the motion of the ship.

The stability of the load depends on the cohesive strength of the bulk solid and whether any yield conditions can be generated in the mass during transport. The possible loading conditions are discussed in the following sections.

3.2 Stress Fields

The stress conditions at some location within the stored mass are depicted in the Mohr diagram of Fig. 12 in which σ_1 and σ_2 are the major and minor principal pressures respectively at the location considered.

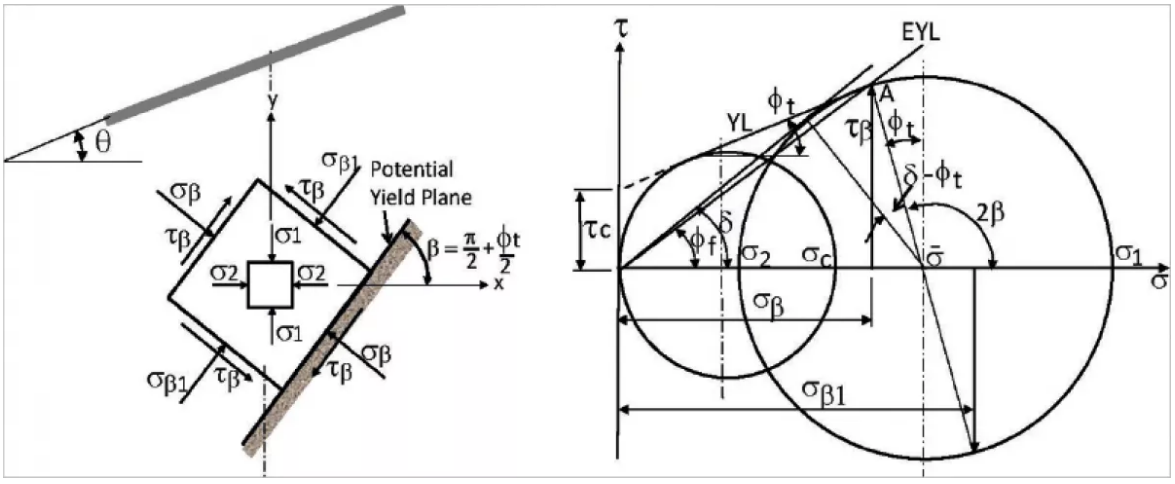

Fig. 12: Stress condition in bulk mass indicating possible plane of failure.

It is assumed that an active state of stress exists and that σ_1 acts vertically being equal in magnitude to the hydrostatic pressure. That is:

$$\sigma_1 = \rho \cdot g \cdot y$$

where:

- ρ is the bulk density,
- *g* is the gravitational acceleration, and
- *y* is the depth below the surface.

In the Mohr diagram of Fig. 12, the point of intersection (Point A) of the yield locus with the Mohr semi-circle through σ_1 and σ_2 defines the stress condition at failure with σ_β being the normal stress and τ_β the shear stress acting on the plane of failure which is inclined at the angle β to the plane of the major principal stress.

From the geometry of Fig. 12, the following relationships can be derived:

$$\sigma_\beta = \frac{\sigma_1}{1+\sin\delta} \cdot \left[1 - \sin\phi_{ti} \cdot \sin\delta\right]$$

$$\tau_\beta = \frac{\sigma_1}{1+\sin\delta} \cdot \left[\cos\phi_{ti} \cdot \sin\delta\right]$$

where:

- δ is the effective angle of internal friction, and
- φ tirepresents the initial static angle of internal friction.

The angle β defining the slope of the yield plane with respect to the principal plane of σ1 is:

$$\beta = 45° + \frac{\phi_{ti}}{2}$$

For a typical coal with an internal friction value of δ = 50 and φ_{ti} = 40°, the angle β can be calculated, resulting in a value of 65°. Additional to the information provided in Fig. 12, an equivalent internal friction angle φ_f is defined by:

$$\phi_f = \tan^{-1}\left(\frac{\tau_\beta}{\sigma_\beta}\right)$$

Substituting Eqs. (4) and (5) into Eq. (7) yields the following expression for φ_f:

$$\phi_f = \tan^{-1}\left(\frac{\cos\phi_t \cdot \sin\delta}{1 - \sin\phi_t \cdot \sin\delta}\right)$$

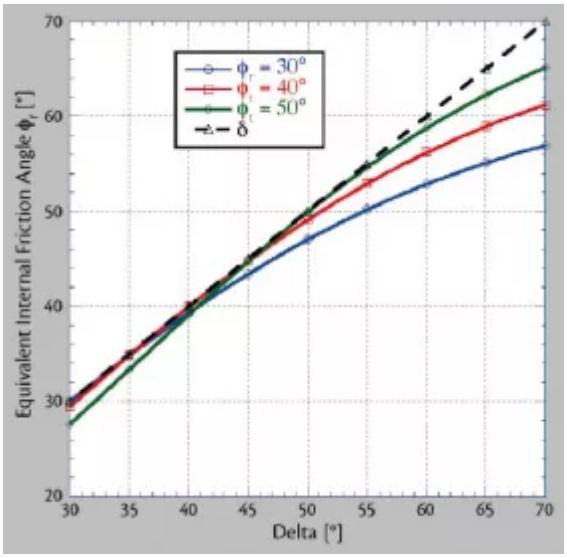

Fig. 13: Equivalent friction angles.

By way of illustration, Fig. 13 shows the variation of the equivalent friction angle φ_f as functions of the effective angle of internal friction δ for a given range of static angles of internal friction φ_{ti}. For comparison purposes, the angle δ is also plotted as is shown by the dotted line. It is noted that for a free flowing bulk solid material, the unconfined yield strength σ_c is generally zero and $\varphi_f = \varphi_{ti} = \delta$.

If, for a given bulk solid and loading configuration, σ_1, δ and φ_{ti} are known, then the stresses τ_β and σ_β on the shear plane may be determined by Eqs. (4) and (5) respectively. Flow property tests enable δand φ_{ti} to be determined as functions of σ_1. However, some uncertainty arises in establishing σ_1. For many cases σ_1 may be estimated from the hydrostatic stress given by Eq. (3). Under these conditions, the plane of failure as defined by β will normally be quite steep. In some occasions, the cohesive shear stress τ_c is required to be expressed as a function of σ_1. Again, from the geometry previously provided in Fig. 12, it may be shown that:

$$\tau_c = K_\tau \cdot \sigma_1$$

with:

$$K_\tau = \frac{1}{1+\sin\delta} \cdot \left[\sin\delta \cdot \left(\cos\phi_{ti} + \sin\phi_{ti} \cdot t \right.\right.$$

Alternatively, the cohesion term τc may also be expressed in terms of the unconfined yield stress σ_c as follows:

$$\tau_c = K_c \cdot \sigma_c$$

with:

$$K_c = 0.5 \cdot \left[\cos\phi_{ti} - \left(1 - \sin\phi_{ti}\right) \cdot \tan\phi_{ti} \right]$$

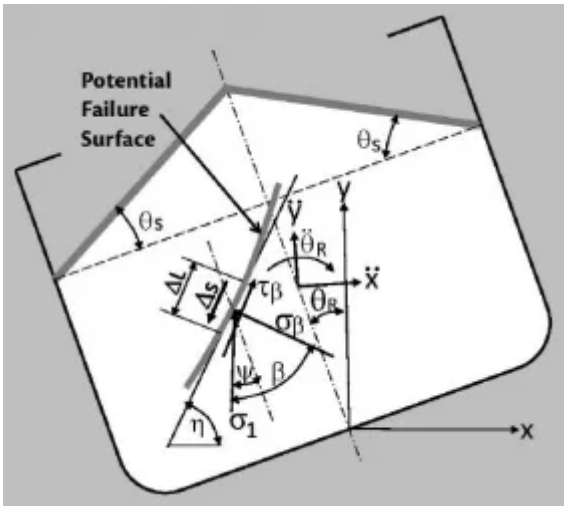

Fig. 14: Stress condition in bulk mass during ship motion.

It is noted that φ_{ti} is the initial value of the static angle of internal friction. Following time consolidation, σ_c will increase to the time consolidation value of the unconfined yield strength σ_{ct} corresponding to the static angle of internal friction φ_t derived from the time yield locus. Very often the value of φ_t is very similar to φ_{ti}.

3.3 Influence of Ship's Motion

When a bulk ship is pitching and rolling, the inertia effects due to the various acceleration components may influence the magnitude and direction of the major consolidation pressure σ_1. The case of rolling motion as depicted in Fig. 14 is reviewed. At the instant considered, the roll angle is θ_R and σ_1 is inclined to the ship's axis at an angle ψ as shown. A potential plane of failure is inclined at an angle $\beta = (\pi/4) + (\phi_t/2)$ to the plane of the major principal pressure σ_1. With respect to the horizontal plane, the possible plane of failure will be inclined at an angle $(\theta_R + \beta - \psi)$. Slip will occur when the shear stress due to the body forces produced by the segment above the shear plane are just equal to the shear stress corresponding to the consolidation condition as given by Eq. (5). That is:

$$\frac{\Delta S}{\Delta L} = \frac{\sigma_1}{1+\sin\delta} \cdot \left(\cos\phi_t \cdot \sin\delta\right)$$

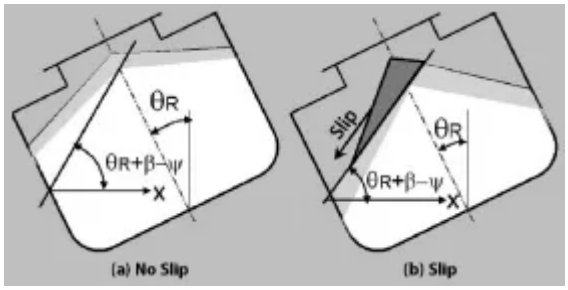

Fig. 15: Safe and possible failure conditions.

The actual failure mode is difficult to predict due to the uncertain consolidation condition. For a cohesive bulk solid, failure is likely to occur along a curved surface. If average values of consolidation are assumed, a rough approximation will be to consider the failure surface as a plane of slope angle (θ_R + β – ψ) with respect to the horizontal axis. Under these conditions failure is less likely to occur if the plane of failure intersects the wall below the surface as in Fig. 15(a). Failure is most likely to occur if the plane of failure is as in Fig. 15(b).

3.4 Consideration of Load Surcharge Zone

Since movement of the bulk solid, if at all, is most likely to be confined to the surface region in the surcharge zone, that portion not constrained by the ship's walls, the condition for stability may be examined by considering slip along the sloping surface. In this case surface slip will occur along a straight inclined plane.

A loosely packed condition near the surface will result in the bulk solid forming a surface slope angle equal to the angle of repose θ. As a guide, θ may be estimated to be equal to the static angle of internal friction φ_t corresponding to zero consolidation pressures.

For the majority of bulk solids ranging from free flowing to highly cohesive, θ will range from about 30 to 40°. However, once the ship commences its journey, the vibration due to the ship's propulsion machinery combined with any whipping, rolling and pitching motion, will result in some settlement of the bulk solid with the surface slope reducing below the natural angle of repose to its transportable surcharge angle θs.

If there is any consolidation near the surface then it is possible for the surface to be inclined at an upper bound stable angle φ_f to the horizontal, φ_f being the equivalent angle of internal friction as defined by Eq. (8) and presented in Fig. 13. For a triangular surcharge as in Fig. 14 where the surface is inclined at a settled transportable surcharge angle θ_s measured with respect to the horizontal, it is possible for no surface movement or slip to occur for roll angles given by:

$$\theta_R \leq \left(\phi_f - \theta_s - \theta_a \right)$$

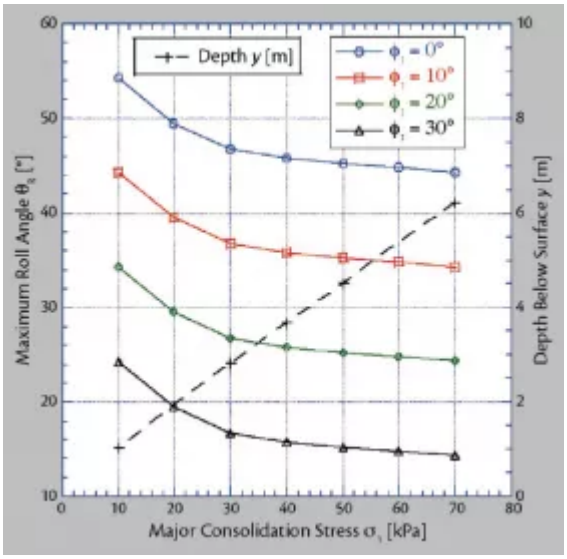

Fig. 16: Maximum roll angles.

where:

- θ_a is an allowance for acceleration inertia effects.

Maximum roll angles have been determined for the coal of Figs. 1, 2 and 3 for a range of transportable surcharge angles from θ_s = 10° to 30°, the results of which are plotted as a function of the major consolidation stress σ_1 in Fig. 16. The corresponding depths below the surface are also shown. Based on Kirby [3], the plotted results assume an acceleration angle θ_a = 5°. If, for example, θ_a = 0, then the maximum roll angle would be 5° larger than those plotted in Fig. 16. The results demonstrate that there is generally a need to trim the free surface on loading in order to prevent material movement for normal roll angles.

4. Ship Load Stability - the Warren Spring Study

The report by Kirby of the Warren Spring Laboratory assumed a circular failure surface for the cohesive case, as is illustrated in Fig. 17 [3]. This assumption is consistent with the classical theory for slope stability in soil mechanics. Kirby defines the non-dimensional parameter *N* as:

$$N = \frac{\tau_c}{\rho \cdot g \cdot L}$$

where:

- τ_c is the cohesion,
- ρ is the bulk density,
- *g* is the gravitational acceleration, and
- *L* is the slope length.

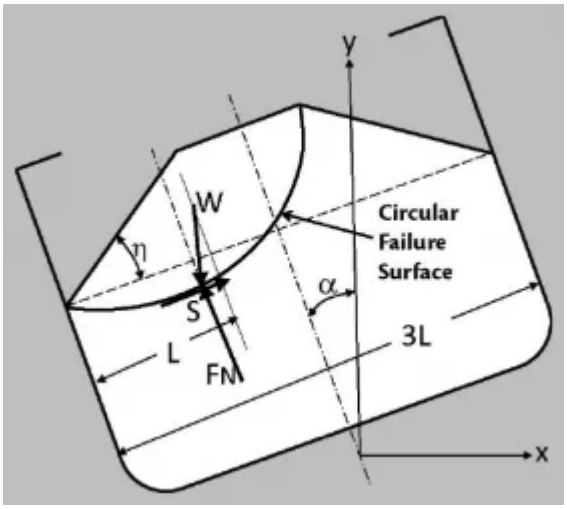

Fig. 17: Stability of bulk cargo [3].

To illustrate the application of this method, an example based on the coal of Figs. 1,2 and 3 is presented with the following assumptions of a 40 m wide ship, a slope length *L* of 13.3 m, a maximum roll angle θ_R of 15° and an assumed acceleration angle θ_a = 5°. Based on the geometry of Fig. 15, for a nominated initial surcharge angle θ_s = 20° and *y* = 4.85 m, the major consolidation pressure σ_1 is approx. 55 kPa. From Figs. 1,2 and 3, this yields a bulk density of ρ = 1.135 t/m^3, an effective internal friction angle δ = 50°, a static internal friction angle φ_t = 44° and an unconfined yield strength σ_c = 16 kPa. From Eqs. (9) to (12), τ_c yields a value of 3.1 kPa and the value of the Kirby non-dimensional factor *N* is 0.021.

From Fig. 46 of Kirby the maximum slope angle is η = 27° which corresponds to a combined roll angle ($\theta_R + \theta_a$) of 20° [3]. For comparison purposes, applying the method described in Section 4.4 shows that the surcharge angle θ_s (or η) is 27°, the maximum combined roll angle ($\theta_R + \theta_a$) is 18° and θ_R = 13°. This is reasonably close to the value of 15° previously calculated.

5. Concluding Remarks

As discussed in this article, the objective of safe ocean transport of bulk cargoes by large bulk ships is vitally dependent on the stability of the cargo under the influence of the rolling, pitching and yawing motion of the ship and the transmission of vibration from the ship’s engine and propulsion machinery as well as wave motion induced whipping. A brief review of the bulk material test procedures recommended by the International Maritime Organisation (IMO) has been presented. The limitations and empirical nature of these tests has been highlighted. The application of the well proven flow property tests and associated analytical and design procedures, widely accepted in the field of bulk solids handling, to bulk ship transportation has been demonstrated.